

Published in final edited form as:

*Bioorg Med Chem Lett.* 2012 September 15; 22(18): 5948–5951. doi:10.1016/j.bmcl.2012.07.062.

## ***N*-Benzoyl anthranilic acid derivatives as selective inhibitors of aldo–keto reductase AKR1C3**

Maša Sinreih<sup>a</sup>, Izidor Sosi<sup>b</sup>, Nataša Berani<sup>a</sup>, Samo Turk<sup>b</sup>, Adegoke O. Adeniji<sup>c</sup>, Trevor M. Penning<sup>c</sup>, Tea Lanišnik Rižner<sup>a</sup>, and Stanislav Gobec<sup>b,\*</sup>

<sup>a</sup>Institute of Biochemistry, Medical Faculty, University of Ljubljana, Ljubljana, Slovenia

<sup>b</sup>Faculty of Pharmacy, University of Ljubljana, Ljubljana, Slovenia

<sup>c</sup>Department of Pharmacology and Center of Excellence in Environmental Toxicology, Perelman School of Medicine, University of Pennsylvania, Philadelphia, PA, USA

### **Abstract**

Human aldo–keto reductases AKR1C1–AKR1C3 are involved in the biosynthesis and inactivation of steroid hormones and prostaglandins and thus represent attractive targets for the development of new drugs. We synthesized a series of *N*-benzoyl anthranilic acid derivatives and tested their inhibitory activity on AKR1C enzymes. Our data show that these derivatives inhibit AKR1C1–AKR1C3 isoforms with low micromolar potency. In addition, five selective inhibitors of AKR1C3 were identified. The most promising inhibitors were compounds **10** and **13**, with IC<sub>50</sub> values of 0.31 μM and 0.35 μM for AKR1C3, respectively.

### **Keywords**

Anthranilic acid; AKR1C3 inhibitors; Anticancer agents

Human aldo–keto reductases AKR1C1–AKR1C4 are involved in the biosynthesis and inactivation of steroid hormones, neurosteroids, prostaglandins, products of lipid peroxidation and xenobiotics. These AKR1C isoenzymes reduce carbonyl containing substrates to alcohols and also act as 3-keto, 17-keto and 20-ketosteroid reductases to varying extents. In this manner, they regulate the activity of androgens, estrogens, progesterone and the occupancy and activation of their corresponding nuclear receptors.<sup>1,2</sup> They possess a broad spectrum of physiological roles, but when differentially expressed they are also involved in different pathophysiological conditions, such as hormone-dependent and independent cancers for example prostate cancer,<sup>3–8</sup> other hormone-dependent diseases,<sup>9</sup> depression, epilepsy and neurodegenerative diseases.<sup>2</sup> These enzymes, and especially AKR1C1 and AKR1C3, thus represent attractive targets for the development of new drugs. As AKR1C enzymes share more than 86% sequence identity at the amino acid level and interestingly, AKR1C1 and AKR1C2 differ in only one residue in the active site (Leu/Val54), development of specific inhibitors is a challenging task.

Anthranilic acid derivatives have been known as good inhibitors of AKR1C isoenzymes, with  $K_i$  values in low micromolar or nanomolar range. Almost 30 years ago, Penning and Talalay showed that indomethacin and mefenamic acid, nonselective NSAIDs, strongly inhibit rat liver hydroxysteroid dehydrogenase AKR1C9, a model for human AKR1C isoenzymes.<sup>10</sup> Other nonselective NSAIDs and selective COX-2 inhibitors also proved to be potent inhibitors of AKR1C isoenzymes.<sup>3,11</sup> This inhibition of AKR1C enzymes by NSAIDs may thus explain the known antineoplastic effects of these drugs. To confirm the hypothesis on involvement of AKR1C isoenzymes in COX-independent anti-proliferative effects, Penning et al. developed selective inhibitors of AKR1Cs based on *N*-phenylanthranilic acid and cholanic acid with  $IC_{50}$  values in low  $\mu$ M range.<sup>3</sup> Recently, we synthesized a series of *N*-benzoyl anthranilic acid derivatives as inhibitors of penicillin binding proteins.<sup>12</sup> Due to their structural similarities to several known inhibitors of AKR1C enzymes, we tested their inhibitory activity on AKR1C enzymes.<sup>13,14</sup> We demonstrated that these derivatives inhibit AKR1C isoenzymes in the low micromolar range. In addition, 5 compounds were found to be selective inhibitors of AKR1C3.

The compounds were synthesized by the formation of the amide bond between carboxylic group of benzoic acid derivatives and the amino moiety of *C*-protected anthranilic acids. The carboxylic acid groups were converted into acid chlorides using  $SOCl_2$ , followed by the addition of the corresponding *C*-protected anthranilic acid derivatives. The esters were subsequently deprotected with alkaline hydrolysis and where necessary an aromatic  $NO_2$  group was reduced into their corresponding amine by catalytic hydrogenation to obtain the target compounds **1–16**. The general experimental procedures for the synthesis of compounds presented in Table 1 and their spectroscopic properties are described in Ref.<sup>12</sup> The detailed synthetic procedure and the spectroscopic data of a representative compound (**11**) are described in note.<sup>15</sup>

Screening of the compounds against recombinant AKR1C1–AKR1C4<sup>16</sup> gave the results presented in Table 1. We found that compounds that possessed either  $NO_2$  (**1–4**) or  $NH_2$  group (**5–7**) at the *meta* position of B ring ( $R^4 = NO_2$  or  $NH_2$ ) and in addition contained different substituents on the anthranilic acid (A) ring were inactive on all AKR1C isoforms. The only exception was compound **8** that had an additional fluorine atom positioned *ortho* with respect to the  $NO_2$  group on the ring B ( $R^4 = NO_2$ ,  $R^5 = F$ ). It exhibited quite potent inhibitory activity against AKR1C1 and AKR1C2 with  $IC_{50}$  values of 8.4  $\mu$ M and 15.6  $\mu$ M, respectively, whereas no AKR1C3 isoform inhibition was observed.

AKR1C3 inhibition was, however, achieved with compounds **9–13**. On the basis of these results we were able to postulate an initial structure–activity relationship for 1C3 isoform inhibition. We found that the presence of the hydroxy group at the *meta* position on the B ring ( $R^4 = OH$ , compounds **9–13**) was essential for selective AKR1C3 inhibition. However, if the hydroxyl group was transformed into an ethoxy ( $R^4 = OEt$ , compound **14**) or butoxy ( $R^4 = OBu$ , compound **15**) moiety, the inhibition shifted towards AKR1C1–C2 isoforms, whereas inhibition of AKR1C3 was almost completely lost. The importance of the hydroxyl group was also confirmed when we compared the inhibitory activities of compounds **2** (3.4% AKR1C3 inhibition) and **3** (3.5% AKR1C3 inhibition), bearing a  $NO_2$  group at the *meta* position on B ring ( $R^4 = NO_2$ ), with their corresponding hydroxy analogs **10** ( $IC_{50} =$

2.2  $\mu\text{M}$ ) and **11** ( $\text{IC}_{50} = 5.2 \mu\text{M}$ ). The same pattern was observed when inhibitory potency of compounds **5** and **6** were compared to the inhibitory potency of compounds **9** and **11**. The latter two compounds possessed a OH group ( $\text{R}^4 = \text{OH}$ ) instead of a  $\text{NH}_2$  moiety at the *meta* position of B ring ( $\text{R}^4 = \text{NH}_2$ ); again this substitution led to increased AKR1C3 inhibitory potency (Table 1). We also found that the substitution on the anthranilic acid (A) ring does not play a significant role in AKR1C3 inhibition as the inhibitory potencies of compounds **9–13** which bear variable substituents on this ring gave comparable  $\text{IC}_{50}$  values ranging from 1.9 to 12.7  $\mu\text{M}$ . However, due to some subtle differences in the  $\text{IC}_{50}$  values we hypothesized that introduction of a large bromine atom to the *meta* position on the A ring ( $\text{R}^1 = \text{Br}$ ) to yield compound **13**, would produce a more potent inhibitor. Compound **13** was found to have an  $\text{IC}_{50}$  value of 1.9  $\mu\text{M}$  for AKR1C3 (Table 1). Compound **16** inhibited all three isoforms 1C1–1C3, with  $\text{IC}_{50}$ s of 3.2, 6.5, and 7.5  $\mu\text{M}$ , respectively.

Those compounds that were selective AKR1C3 inhibitors in the primary screen against 1C1–1C3 isoforms, were subjected to a confirmatory screen which included AKR1C4. These compounds showed even better inhibitory potencies (Table 1), which we assign to differences in assay procedures and conditions.<sup>16</sup> As the  $\text{IC}_{50}$  values for compounds **9–13** were determined on all AKR1C isoforms, we were able to calculate the range of selectivity for the most potent AKR1C3 inhibitors. Here, the most promising compound was **13** with an  $\text{IC}_{50}$  value of 0.35  $\mu\text{M}$  on the AKR1C3 isoform and it exhibited 286-, 180- and 86-fold selectivity for AKR1C3 in comparison with isoforms 1C1, 1C2 and 1C4, respectively (Table 1). Also, compound **10** seems very promising as it was similarly selective as compound **13**. These two inhibitors of AKR1C3 are amongst the most potent selective non-steroidal inhibitors published so far. The only significantly more potent inhibitors were steroidal lactones, which were active in nanomolar concentrations. However, their selectivity over other AKR1C isoforms has not been demonstrated.<sup>17,18</sup>

To enhance our understanding of the results of enzymatic assays and to confirm our postulated SAR we used molecular docking<sup>19,20</sup> to predict the hypothetical binding pose of compound **13** in the active site of AKR1C3 (PDB code 1S2A).<sup>21</sup> The predicted binding pose of **13** showed several important interactions. With its carboxyl group, it was predicted to form H-bonds with the catalytic tetrad members Tyr55 and His117 (Fig. 1). Surprisingly, the other part of compound **13** (ring B) was predicted to bind to the SP3 binding pocket<sup>21,22</sup> composed of Tyr24, Glu192, Ser221 and Tyr305 which is similar to the binding mode of indomethacin.<sup>23</sup> The 3-hydroxy group of ring B was predicted to form H-bonds with Ser221 and the backbone nitrogen of Gln222. Additional  $\pi$ - $\pi$  interactions were predicted to form between ring B and Tyr24. The interactions with SP3 binding pocket seem to be crucial for good AKR1C3 inhibitory activity in this series as compounds **14** and **15** with alkylated hydroxy groups exhibited lower AKR1C3 inhibition, most probably due to the loss of H-bonds with Ser221 and Gln222. It is interesting to note that this hypothetical binding pose is different from binding poses of highly related *N*-phenylaminobenzoate,<sup>22</sup> which were shown to occupy the SP1 binding pocket (formed by Ser118, Asn167, Phe306, Phe311, and Tyr319), similarly as flufenamic acid.<sup>23</sup>

To conclude, we have evaluated a series of *N*-benzoyl anthranilic acid derivatives for their inhibition of aldo-keto reductases AKR1C1–C4 and discovered some new selective

inhibitors of AKR1C3, an important drug target. The results represent an important basis for the synthesis of next generation of AKR1C3 inhibitors. As the synthetic procedures to obtain structurally related derivatives are very straightforward, we are certain that further improvements can be achieved. Both phenyl rings (A and B) offer several possibilities for the introduction of new functionalities at different positions. The most promising way forward is to synthesize compounds which retain moieties that seem to play an important role for selective AKR1C3 inhibition and to explore the SAR of different compounds with varied substitution patterns on the anthranilic acid phenyl ring. These optimized compounds will have the potential to be further developed into drug candidates for treatment of hormone dependent and independent forms of prostate and breast cancers.

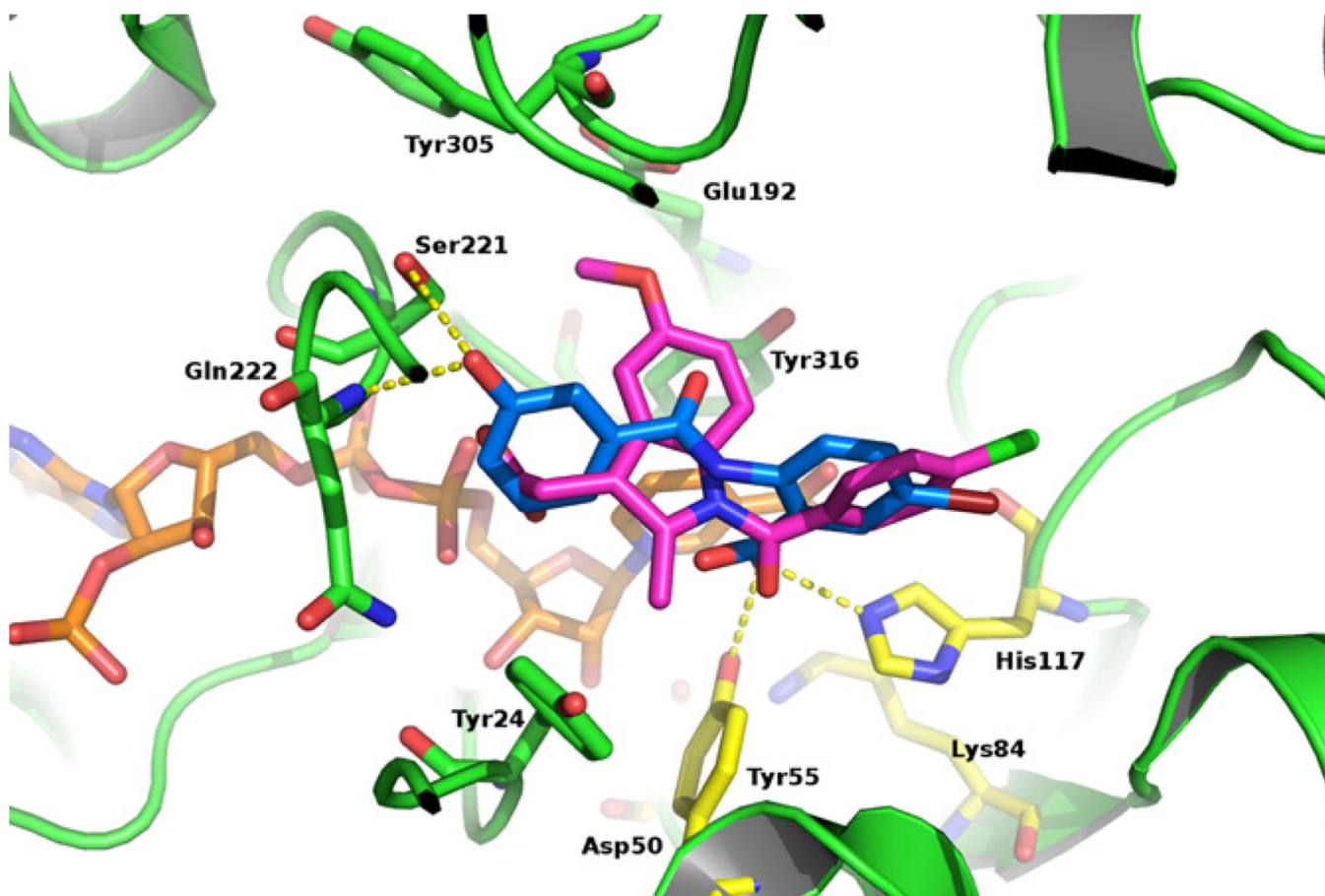
## References and notes

1. Barski OA, Tipparaju SM, Bhatnagar A. *Drug. Metab. Rev.* 2008; 40:553. [PubMed: 18949601]
2. Penning TM, Drury JE. *Arch. Biochem. Biophys.* 2007; 464:241.
3. Bauman DR, Rudnick SI, Szewczuk LM, Jin Y, Gopishetty S, Penning TM. *Mol. Pharmacol.* 2005; 67:60. [PubMed: 15475569]
4. Wang S, Yang Q, Fung KM, Lin HK. *Mol. Cell. Endocrinol.* 2008; 289:60.
5. Adeniji AO, Twenter BM, Byrns MC, Jin Y, Winkler JD, Penning TM. *Bioorg. Med. Chem. Lett.* 2011; 21:1464. [PubMed: 21277203]
6. Desmond JC, Mountford JC, Drayson MT, Walker EA, Hewison M, Ride JP, Loung QT, Hayden RE, Vanin EF, Bunce CM. *Cancer Res.* 2003; 63:505. [PubMed: 12543809]
7. Dozmorov MG, Azzarelo JT, Wren JD, Fung KM, Yang Q, Davis JS, Hurst RE, Culkin DJ, Penning TM, Lin HK. *BMC Cancer.* 2010; 10:672. [PubMed: 21134280]
8. Lewis MJ, Wiebe JP, Heathcote JG. *BMC Cancer.* 2004; 4:27. [PubMed: 15212687]
9. Hevir N, Vovk K, Pucelj MR, Rižner TL. *Chem.-Biol. Interact.* 2011; 191:217. [PubMed: 21232532]
10. Penning TM, Talalay P. *Med. Sci.* 1983; 80:4504.
11. Gobec S, Broži P, Rižner TL. *Bioorg. Med. Chem. Lett.* 2005; 15:5170. [PubMed: 16183274]
12. Sosi I, Turk S, Sinreih M, Trošt N, Verlaine O, Amoroso A, Zervosen A, Luxen A, Joris B, Gobec S. *Acta Chim. Slov.* 2012; 59:380.
13. Broži P, Šmuc T, Gobec S, Rižner TL. *Mol. Cell. Endocrinol.* 2006; 259:30. [PubMed: 16962702]
14. Broži P, Turk S, Lanišnik-Rižner T, Gobec S. *Curr. Med. Chem.* 2011; 18:2554. [PubMed: 21568892]
15. Experimental procedure for the preparation of methyl 2-(3-hydroxybenzamido)-4,5-dimethoxybenzoate: To a solution of 3-hydroxybenzoic acid (138.12 mg, 1.0 mmol) in CH<sub>2</sub>Cl<sub>2</sub> (10 mL), pyridine (99 mg, 1.25 mmol) and SOCl<sub>2</sub> (773 mg, 6.5 mmol) were slowly added. After stirring at 45 °C for 2 h, the solvent was removed under reduced pressure. The reaction mixture was dissolved in toluene, and then methyl 2-amino-4,5-dimethoxybenzoate (264 mg, 1.25 mmol) was added. The reaction mixture was stirred at 100 °C for 3 h. After the reaction was complete (monitored by TLC), the solvent was evaporated, then an aqueous solution of Na<sub>2</sub>CO<sub>3</sub> (10%, 10 mL) was added, and the aqueous layer was extracted with CH<sub>2</sub>Cl<sub>2</sub> (3 × 10 mL). The combined organic phases were washed with brine (2 × 20 mL) and dried over Na<sub>2</sub>SO<sub>4</sub>. The solvent was evaporated, and the pure product was obtained by crystallization from EtOH. Yield, 71% (235 mg). Experimental procedure for the preparation of 2-(3-hydroxybenzamido)-4,5-dimethoxybenzoic acid (**11**): To a stirred solution of the methyl 2-(3-hydroxybenzamido)-4,5-dimethoxybenzoate (165 mg, 0.5 mmol) in dioxane/THF mixture (1:1, 2 mL), 1 M NaOH (1 mL) was added, and the reaction mixture stirred until the starting material had completely reacted (monitored by TLC). The solvent was then evaporated under reduced pressure, the residue diluted with H<sub>2</sub>O (10 mL), and washed with EtOAc (2 × 10 mL). The aqueous phase was acidified to pH 2 using 1 M HCl, and extracted with EtOAc (3 × 10 mL). The combined organic phases were washed with brine (3 × 10 mL), then dried over Na<sub>2</sub>SO<sub>4</sub>, filtered, and evaporated to dryness, to

provide compound **11**. Yield, 74% (117 mg). Spectroscopic data for 2-(3-hydroxybenzamido)-4,5-dimethoxybenzoic acid (**11**): White solid; Yield: 51% (2 steps);  $R_f$  0.49 (CH<sub>2</sub>Cl<sub>2</sub>/MeOH/AcOH = 9/1/0.1); Mp: 245.0–248.0 °C; <sup>1</sup>H NMR (400 MHz, DMSO-*d*<sub>6</sub>): δ 3.79 (s, 3H, OCH<sub>3</sub>), 3.87 (s, 3H, OCH<sub>3</sub>), 6.95–7.03 (m, 1H, Ar-H), 7.32–7.39 (m, 3H, Ar-H), 7.49 (s, 1H, Ar-H), 8.52 (s, 1H, Ar-H), 9.91 (br s, 1H, *NHCO*), 13.51 (br s, 1H, *COOH*); <sup>13</sup>C NMR (100 MHz, DMSO-*d*<sub>6</sub>): δ 55.54 (2C), 102.98, 107.47, 112.83, 113.84, 117.15, 119.01, 129.95, 135.95, 136.98, 143.58, 153.25, 157.76, 164.41, 169.72; HRMS (ESI) *m/z* calcd for C<sub>16</sub>H<sub>15</sub>N<sub>2</sub>O<sub>5</sub> [M+H]<sup>+</sup> 318.0978, found 318.0969; HPLC purity: 95.54%, retention time: 14.06 min. HPLC was performed on an Agilent Eclipse C18 column (4.6 × 50 mm, 5 μm), with a flow rate of 1.0 mL/min, detection at 254 nm, and an eluent system of: A = 0.1% TFA in H<sub>2</sub>O; B = MeOH. The following gradient was applied: 0–3 min, 40% B; 3–18 min, 40% B → 80% B; 18–23 min, 80% B; 23–30 min, 80% B → 40% B. The run time was 30 min, at a temperature of 25 °C.

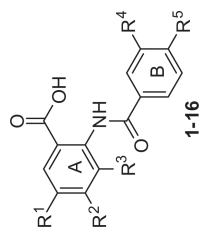
16. The primary inhibition assay: Recombinant enzymes AKR1C1–AKR1C3 were prepared as described previously (13). Inhibition of the individual isoenzyme was monitored spectrophotometrically in the direction of oxidation, with 1-acenaphthenol as a substrate and NAD<sup>+</sup> as a coenzyme. Reaction was followed by measuring the increase in NADH absorbance ( $\epsilon_{\lambda 340} = 6220 \text{ M}^{-1}\text{cm}^{-1}$ ) in the absence and presence of each of the compound. The assays were carried out in a 300 μL volume that included 100 mM phosphate buffer (pH 9.0), 0.005% triton X-114 and 5% DMSO as a co-solvent. A substrate concentration of 30 μM ( $K_m$ ), 60 μM ( $K_m$ ) and 100 μM ( $<K_m$ ) and an enzyme concentration of 0.1 μM, 0.3 μM, and 1.5 μM were used for assays with AKR1C1, AKR1C2 and AKR1C3, respectively, in the presence of 2.3 mM NAD<sup>+</sup>. Screening was performed at 10 μM concentration of compounds. For compounds that showed more than 30% AKR1C1–AKR1C3 inhibition, IC<sub>50</sub> values were determined. The measurements were performed on a Biotek PowerWave XS microplate readers with initial velocities calculated, and the IC<sub>50</sub> values were determined graphically, using GraphPad Prism Version 4.00 (GraphPad Software, Inc.). *The secondary inhibition assay*: The potency of the compounds was determined also by measuring their ability to inhibit the NADP<sup>+</sup> dependent oxidation of *S*-(+)-1,2,3,4-tetrahydro-1-naphthol (*S*-tetralol) catalyzed by AKR1C1–AKR1C4 enzymes. The continuous assay was conducted using a 96-well plate format and the reaction measured the appearance of NADPH fluorimetrically (Exc/Emi, 340/460 nm) on a BIOTEK Synergy 2 Multimode plate reader. The assay mixture consisted of 100 mM phosphate buffer, pH 7.0, *S*-tetralol (in DMSO), inhibitor (in DMSO), 200 μM NADP<sup>+</sup>, and purified recombinant enzyme to give a total volume of 200 μL, and 4% DMSO. The concentration of *S*-tetralol used in the assays for each AKR1C isoform was equal to the  $K_m$  value for the respective enzyme. The  $K_m$  value obtained for *S*-tetralol for AKR1C1, AKR1C2, AKR1C3 and AKR1C4 under the same experimental conditions are 8 μM, 22.5 μM, 165 μM, and 25 μM, respectively. Enzyme concentrations used for AKR1C1, AKR1C2, AKR1C3 and AKR1C4 were 111 nM, 86 nM, 95 nM and 184 nM, respectively. Initial velocity from progress curves was calculated with the GEN5 software. Inhibition data were fit using Grafit 5.0 [ $y = (\text{range})/(1+I/IC_{50})_s + \text{background}$ ] to give the IC<sub>50</sub> values.
17. Bydal P, Luu-The V, Labrie F, Poirier D. Eur. J. Med. Chem. 2009; 44:632. [PubMed: 18472187]
18. Qiu W, Zhou M, Mazumdar M, Azzi A, Ghanmi D, Luu-The V, Labrie F, Lin S-X. J. Biol. Chem. 2007; 282:8368. [PubMed: 17166832]
19. For docking experiments, FlexX 3.1 (BiosolveIT GmbH) (20) was used together with the crystal structure of AKR1C3 (PDB code 1S2A (21)). The active site was defined as the volume of the enzyme within 6 Å from co-crystallized ligand. The cofactor NADP<sup>+</sup> was retained in the active site. For the base placement, Triangle Matching was used: this programme generated the maxima of 200 solutions per iteration and 200 per fragmentation. The docking procedure was validated since FlexX was able to reproduce the conformation of cocrystallized ligand.
20. Rarey M, Kramer B, Lengauer T, Klebe G. J. Mol. Biol. 1996; 261:470. [PubMed: 8780787]
21. Byrns MC, Jin Y, Penning TM. J. Steroid. Biochem. Mol. Biol. 2011; 125:95. [PubMed: 21087665]
22. Chen M, Adeniji AO, Twenter BM, Winkler JD, Christianson DW, Penning TM. Bioorg. Med. Chem. Lett. 2012; 22:3492. [PubMed: 22507964]
23. Lovering AL, Ride JP, Bunce CM, Desmond JC, Cummings SM, White SA. Cancer Res. 1802; 2004:64.



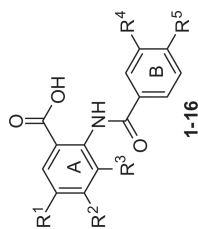


**Figure 1.** The predicted binding conformation of compound **13** (blue) in the active site of AKR1C3. Relevant enzyme residues are shown as green sticks, the catalytic tetrad is presented as yellow sticks, the co-crystallized indomethacin as magenta sticks and the cofactor as orange sticks. Compound **13** occupies a portion of the SP3 pocket which up until now has only been occupied by indomethacin.

Table 1

Inhibitory activities for compounds **1–16**<sup>a</sup>

	R <sup>1</sup>	R <sup>2</sup>	R <sup>3</sup>	R <sup>4</sup>	R <sup>5</sup>	AKR1C1 inhibition <sup>b,c</sup> (%)	AKR1C2 inhibition <sup>b,c</sup> (%)	AKR1C3 inhibition <sup>b,c</sup> (%)	AKR1C4 inhibition <sup>c</sup> (%)
1	OH	H	H	NO <sub>2</sub>	H	NI	31.6 <sup>d</sup>	1.9	n.d.
2	Cl	H	H	NO <sub>2</sub>	H	NI	23.4	3.4	n.d.
3	OMe	OMe	H	NO <sub>2</sub>	H	22.2	NI	3.5	n.d.
4	Cl	H	Me	NO <sub>2</sub>	H	NI	22.5	NI	n.d.
5	H	H	H	NH <sub>2</sub>	H	8.0	NI	NI	n.d.
6	OMe	OMe	H	NH <sub>2</sub>	H	18.0	20.2	5.6	n.d.
7	OH	H	H	NH <sub>2</sub>	H	9.7	28.7	5.6	n.d.
8	Br	H	H	NO <sub>2</sub>	F	53.2	33.6	5.6	n.d.
9	H	H	H	OH	H	NI	IC <sub>50</sub> = 8.4 μM	IC <sub>50</sub> = 15.6 μM	n.d.
							NI	42.1	n.d.
								IC <sub>50</sub> = 12.7 μM	
10	Cl	H	H	OH	H	17.4	IC <sub>50</sub> = >100 μM <sup>e</sup> (>19) <sup>e</sup>	IC <sub>50</sub> = 5.19 μM <sup>c</sup>	IC <sub>50</sub> = 100 μM <sup>c</sup> (>19) <sup>e</sup>
							6.7	77.8	n.d.
								IC <sub>50</sub> = 2.2 μM	
11	OMe	OMe	H	OH	H	11.8	IC <sub>50</sub> = 50.8 μM <sup>c</sup> (164) <sup>e</sup>	IC <sub>50</sub> = 0.31 μM <sup>c</sup>	IC <sub>50</sub> = 20.1 μM <sup>c</sup> (65) <sup>e</sup>
							29.4	70.2 IC <sub>50</sub> = 5.2 μM	n.d.
							IC <sub>50</sub> = 86.3 μM <sup>cc</sup> (30) <sup>e</sup>	IC <sub>50</sub> = 2.9 μM <sup>c</sup>	IC <sub>50</sub> = 50.9 μM <sup>c</sup> (18) <sup>e</sup>
12	NO <sub>2</sub>	H	H	OH	H	11.8	10.4	87.9 IC <sub>50</sub> = 2.6 μM	n.d.
							IC <sub>50</sub> = 35.2 μM <sup>c</sup> (42) <sup>e</sup>	IC <sub>50</sub> = 0.84 μM <sup>c</sup>	IC <sub>50</sub> = 32.3 μM <sup>c</sup> (38) <sup>e</sup>



R <sup>1</sup>	R <sup>2</sup>	R <sup>3</sup>	R <sup>4</sup>	R <sup>5</sup>	AKR1C1 inhibition <sup>b,c</sup> (%)	AKR1C2 inhibition <sup>b,c</sup> (%)	AKR1C3 inhibition <sup>b,c</sup> (%)	AKR1C4 inhibition <sup>c</sup> (%)
13	Br	H	OH	H	21.6	16.7	89.6 IC <sub>50</sub> = 1.9 μM	n.d. IC <sub>50</sub> = 30.3 μM <sup>c</sup> (86) <sup>e</sup>
14	Br	H	OEt	H	31.9 IC <sub>50</sub> = 20.6 μM	36.8 IC <sub>50</sub> = 63.0 μM <sup>c</sup> (180) <sup>e</sup>	19.1 IC <sub>50</sub> = 0.35 μM <sup>c</sup>	n.d.
15	Br	H	OBu	H	65.9 IC <sub>50</sub> = 4.9 μM	70.5 IC <sub>50</sub> = 17.1 μM	30.4	n.d.
16	H	H	OBu	NO <sub>2</sub>	70.8 IC <sub>50</sub> = 3.2 μM	58.3 IC <sub>50</sub> = 6.5 μM	47.2 IC <sub>50</sub> = 7.5 μM	n.d.

NI, No inhibition observed.

n.d., Not determined.

<sup>a</sup>The data represent the mean value of two independent experiments. Standard deviations were within ±10% of these mean values.

<sup>b</sup>The inhibitory activities at 10 μM of each compound and IC<sub>50</sub> values were determined with the primary assay, first line.

<sup>c</sup>The IC<sub>50</sub> values of the selected 5 compounds were determined with the secondary assay, second line.

<sup>d</sup>The compound precipitated at higher concentrations under assay conditions.

<sup>e</sup>Values in parenthesis, determined on the basis of the secondary assay results, represent fold selectivity for AKR1C3.